

Chemical Science

Accepted Manuscript



This is an *Accepted Manuscript*, which has been through the Royal Society of Chemistry peer review process and has been accepted for publication.

Accepted Manuscripts are published online shortly after acceptance, before technical editing, formatting and proof reading. Using this free service, authors can make their results available to the community, in citable form, before we publish the edited article. We will replace this *Accepted Manuscript* with the edited and formatted *Advance Article* as soon as it is available.

You can find more information about *Accepted Manuscripts* in the [Information for Authors](#).

Please note that technical editing may introduce minor changes to the text and/or graphics, which may alter content. The journal's standard [Terms & Conditions](#) and the [Ethical guidelines](#) still apply. In no event shall the Royal Society of Chemistry be held responsible for any errors or omissions in this *Accepted Manuscript* or any consequences arising from the use of any information it contains.



www.rsc.org/chemicalscience



Semiconductive 3-D Haloplumbate Framework Hybrids with High Color Rendering Index White-Light Emission

Guan-E Wang,^a Gang Xu,^{*a} Ming-Sheng Wang,^a Li-Zhen Cai,^a Wen-Hua Li^a and Guo-Cong Guo^{*a}

Received 00th January 20xx,
Accepted 00th January 20xx

DOI: 10.1039/x0xx00000x

www.rsc.org/

Single-component white light materials may create great opportunity for novel conventional lighting industry and display system; however, the reported color rendering index (CRI) values of them, one of the key parameters for lighting, are less than 90, which does not satisfy the demand in color-critical upmarket applications, such as photography, cinematography, and art galleries. In this work, two semiconductive chloroplumbate (chloride anion of lead(II)) hybrids, obtained by a new inorganic-organic hybrid strategy, show unprecedented 3-D inorganic framework structures and white-light-emitting properties with high CRI values in the 90 range, one of which shows the highest value to date.

Introduction

Multi-functional material possessing both luminescent and semiconductive properties has played critical role in solid-state lighting (SSL) technique.¹ The materials with good electrical properties will enable to convert electricity to light in much higher efficiency and smaller device than conventional incandescent or fluorescent lighting source. Realizing white-light luminescence is the key step for SSL to alternate conventional lighting and display system. The most used method to produce white-light luminescence is multi-component strategy. This strategy includes three ways: one is to excite a yellow phosphor (or multi-phosphors) by a blue (or UV) light-emitting diode (LED); another one is to blend red, green and blue LED;² A third way is to excite a white phosphor by a UV light source.³ Multi-component strategy can provide good color-rendering properties, but suffers from efficiency loss owing to self-absorption as well as emission color changes due to individual phosphor degrades at different rates.⁴ Single-component strategy is an alternative strategy to generate white-light luminescence.⁵ It can overcome the drawbacks in multi-component strategy and has advantages such as improved stability, easier fabrication process, and better color reproducibility.⁶ However, it is still a big challenge to obtain a single-component material with high quality white-light luminescence.

Color rendering index (CRI) is a very important parameter of SSL device and full-color display system.⁷ It describes how well a light source renders the colors of the object comparing

to an incandescent light or daylight. CRI has a scale from 0 to 100 percent and the higher its value, the better color rendering ability. A source with CRI of 70 is acceptable for normal lighting application, while CRI of 80 is needed to human eye-friendly application. Ultra-high CRI (above 90) is required to satisfy the demand in color-critical high-level applications, such as photography, cinematography, art galleries, jewelry, surgery, and cosmetic sales counter. With very high cost, ultra-high CRI multi-component system can be obtained by carefully balancing the emitting intensities of different colors.⁸ However, ultra-high CRI in single-component system has not been reported yet. As far as we known, most reported single-component materials have CRI values less than 85.⁹ The photoluminescence spectrum of single-component white-light emitting phosphor normally shows a very broad peak with fixed ratio of different colors. Therefore, to individually tune the emitting intensities of different colors is very difficult in this case.

Crystalline inorganic-organic hybrid has shown great achievement in single-component white-light emitting,^{5a} but ultra-high CRI has not been realized. In hybrid system, white light is mainly coming from broad emitting of inorganic components.^{9a,9b} One possible way to improve CRI is to involve organic emitting center in hybrid. Hybrid material system normally has weak interaction between inorganic and organic components which make it possible to design a hybrid with very weak electronic communication between inorganic and organic components. Therefore, when inorganic and organic components are selected to separately have blue and yellow / orange emitting centers, and partially overlapped excitation band, it would result: 1) the overlapped excitation band can activate blue and yellow / orange emission synchronously; 2) multi-emitting-centers are independently tunable to balance the ratio of the emissions of different colors by shifting exciting wavelength. In this manner, white-light emission of this hybrid material can be realized and CRI of it can be tuned

^a State Key Laboratory of Structural Chemistry, Fujian Institute of Research on the Structure of Matter, Chinese Academy of Sciences, Fuzhou, Fujian 350002, P. R. China

† Footnotes relating to the title and/or authors should appear here.

Electronic Supplementary Information (ESI) available: [details of any supplementary information available should be included here]. See DOI: 10.1039/x0xx00000x

to high value. Moreover, the inorganic component can be selected to provide good electrical properties for hybrid material.¹⁰ Thus, a multifunctional hybrid with both good conductivity and interesting light emission might be designed and created.

Here, we report a single-component white-light emitting compound with CRI as high as 96, which is the highest value to date. By inorganic-organic hybrid strategy, two crystalline hybrids, (H₂DABCO)(Pb₂Cl₆) (**1**) and (H₃O)(Et₂DABCO)₈(Pb₂₁Cl₅₉) (**2**), (DABCO = 1,4-diazabicyclo[2.2.2]-octane; Et = ethyl) were synthesized. Single crystal X-ray diffraction measurement revealed their unique lead halide based three-dimensional (3-D) inorganic framework structures. These two hybrids have independently tunable organic blue emitting component and inorganic yellow / orange emitting component for high CRI white-light emitting. Photoluminescence (PL) study showed compound **1** has cold-white-light emitting with CRI of 96 and compound **2** has warm-white-light emitting with CRI of 88, respectively. In addition, electrical studies of **1** and **2** revealed their typical semiconductive properties.

Results and discussion

Colorless crystals of **1** and **2** were obtained by the solvothermal treatment of PbCl₂ and DABCO in ethanol and *n*-butanol, respectively. Detail of the synthesis is shown in supporting information (SI). Their phase purity was verified by elemental analysis and powder X-ray diffraction (PXRD) determination (see the experimental section and Fig. S1 in the SI).

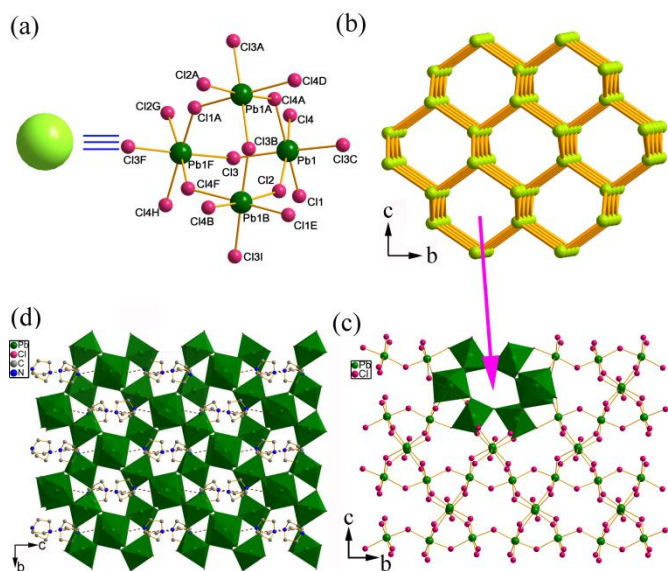


Fig. 1. For **1**: a) Topological node of the Pb₄Cl₁₈ cluster; b) Topological diamond structure of the (Pb₂Cl₆)²⁻ ions; c) Structures of the (Pb₂Cl₆)²⁻ framework viewed along the *a* axis, where parts of the Pb octahedra are shown as polyhedra; d) Crystal structure of compound **1** viewed along the *a* direction. Hydrogen atoms are omitted for clarity. The organic (H₂DABCO)²⁺ cations were accommodated in the hexagonal channels through N–H···Cl (with a mean N1···Cl3 separation of 3.263(11) Å, and a mean N1–H···Cl3 angle of 139.1(7)°) hydrogen bonding interactions. Symmetric code: A: 1.5–*y*, 0.5+*x*, –0.25+*z*; B: –1+*y*, 1+*x*, –1+*z*; C: 0.5+*x*, 2.5–*y*, –0.75+*z*; D: 1–*x*, 2–*y*, –0.5+*z*; E: 1–*x*, 3–*y*, –0.5+*z*; F: –0.5+*x*,

2.5+*y*, –0.75+*z*; G: –0.5+*x*, 2.5+*y*, –0.75+*z*; H: –1.5+*y*, 1.5–*x*, 0.25+*z*; I: 1–*y*, 2–*x*, –0.5+*z*; J: 1.5–*y*, 1.5+*x*, –0.25+*z*.

Single-crystal X-ray diffraction analysis reveals that compound **1** crystallizes in the tetragonal space group *P*4₃2₁2. The structure of **1** is composed of a unique 3-D (Pb₂Cl₆)²⁻ framework hosting organic (H₂DABCO)²⁺ cations (Fig. 1d). Notably, metal halide-based hybrid normally has 0-D, 1-D or 2-D inorganic structure; the 3-D inorganic framework structures were rarely obtained previously.¹¹ As shown in Fig. S2, there are one crystallographically independent Pb atom and four Cl atoms, and each Pb atom is situated in a slightly distorted octahedral coordination environment. From the topological view of point, four corner shared PbCl₆ octahedra form a Pb₄Cl₁₈ cluster as a node (Fig. 1a), and then this node connects with four neighboring ones to form a 3-D diamond structure. The whole net has a 6-connected topology with the point symbol of (3⁶.6⁶.7³) (Fig. 1b). This 3-D inorganic framework shows alternately hexagonal channels along the *a* and *b* directions, which has a window of 9.215(4) × 5.470(3) Å² (Fig. 1c, S3). The organic (H₂DABCO)²⁺ cations were accommodated in the hexagonal channels through N–H···Cl hydrogen bonding interactions (Fig. 1d).

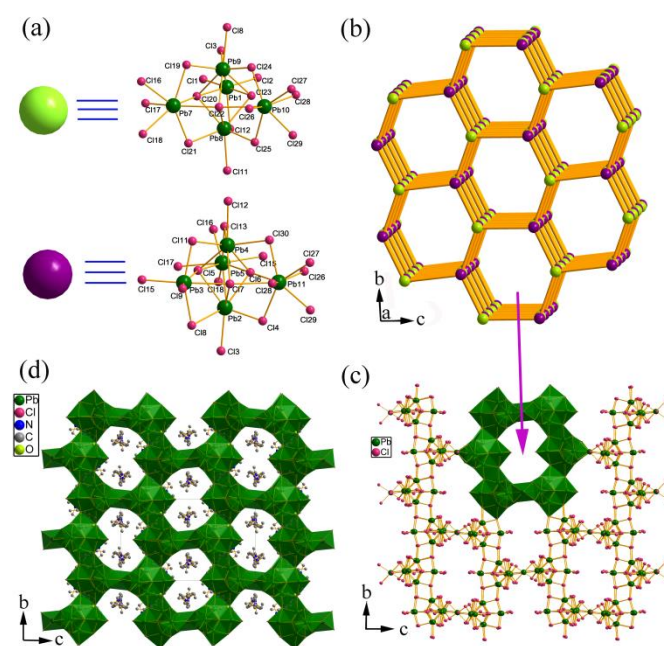


Fig. 2. For **2**: a) Topological node of the Pb₂Cl₁₈ cluster; b) Topological structure of the (Pb₂₁Cl₅₉)²⁻ ions; c) Structures of the (Pb₂₁Cl₅₉)²⁻ framework viewed along the *a* axis, where parts of the Pb octahedra are shown as polyhedra; d) Crystal structure of compound **2** viewed along the *a* direction. Hydrogen atoms are omitted for clarity.

Compound **2** crystallizes in the monoclinic space group *P*2(1)/*c*, which is composed of another unprecedented 3-D (Pb₂₁Cl₅₉)¹⁷⁻ framework as well as organic (Et₂DABCO)²⁺ dications and protonated water molecules (Fig. 2d). Different from the protonated DABCO dications in **1**, the DABCO molecule in **2** is ethylated during the synthesis. This *in-situ* *N*-alkylation has been well developed in our group for synthesizing metal halide-based hybrids.¹² (Et₂DABCO)²⁺ is

larger than $(\text{H}_2\text{DABCO})^{2+}$ dication in size, which results in larger channels in the 3-D inorganic framework of **2**. There are eleven crystallographically independent Pb atoms in the structure and they are situated in a distorted octahedral or mono-capped prismatic coordination environment. Two different trigonal bipyramid shaped $\text{Pb}_5\text{Cl}_{18}$ clusters are simplified to two kinds of nodes to the topological view of point (Fig. 2a). They have differences in the coordination environment of Pb, and connect with each other through three Cl bridged atoms (Cl16, Cl17, Cl18) at *a* direction and two bridged Cl atoms (Cl11, Cl12) at the *b* direction (Fig. S4). One node connects with three other neighboring nodes leads to an alveolate layer in the *bc* plane (Fig. 2b, 2c). These alveolate layers are further connected by the Pb6-centered octahedron to form a 3-D inorganic framework with 1-D channels in the *a* direction (Fig. S5). This structure has 4,5-connected net with the point symbol of $(3.4^4.5^2.6^3)_4(3^2.6^2.7^2)$. The 3-D inorganic framework showed splayed channels with windows of $12.656(15) \times 10.333(7) \text{ \AA}^2$ (Fig. S5). $(\text{Et}_2\text{DABCO})^{2+}$ dications and protonated water molecules are located in the channels and contact with 3-D $(\text{Pb}_{21}\text{Cl}_{59})^{17-}$ anions through Coulomb interactions (Fig. 2d).

Lead halide and its inorganic-organic hybrid normally are interesting p-type semiconductive materials. 3-D lead halide-based hybrid materials have created impressive progress in solar cells with over 19% solar conversion efficiencies in recent years.¹³ The electrical properties of **1** and **2** were determined by a two-probe direct current (DC) method with the pressed pellets of powdered samples from 30 to 170 °C. In an I-V curve, the steeper slope indicates the higher conductivity of a sample. As shown in figure S6a and S6c, the conductivity of **1** is $2.18 \times 10^{-7} \text{ S}\cdot\text{cm}^{-1}$ at 30 °C, which gradually increases by raising temperature and reaches to $2.13 \times 10^{-5} \text{ S}\cdot\text{cm}^{-1}$ at 170 °C. The variety of the conductivity of **2** has the similar trend to that of **1**. It has conductivity of $2.83 \times 10^{-7} \text{ S}\cdot\text{cm}^{-1}$ at 30 °C and $2.24 \times 10^{-3} \text{ S}\cdot\text{cm}^{-1}$ at 170 °C, respectively. Both the values and the trend that the conductivity increases by raising temperature are very typical for a semiconductive material. The semiconductive properties of these hybrids should originate from the 3-D inorganic frameworks in the structure, which has been observed in other compounds in the same hybrid material family.¹⁴ From optical absorption measurement (Fig. S7), compound **2** has smaller energy gap (*E_g*) than that of **1**. This might be an important reason why compound **2** has more significant change of the conductivity when varying ambient temperature.

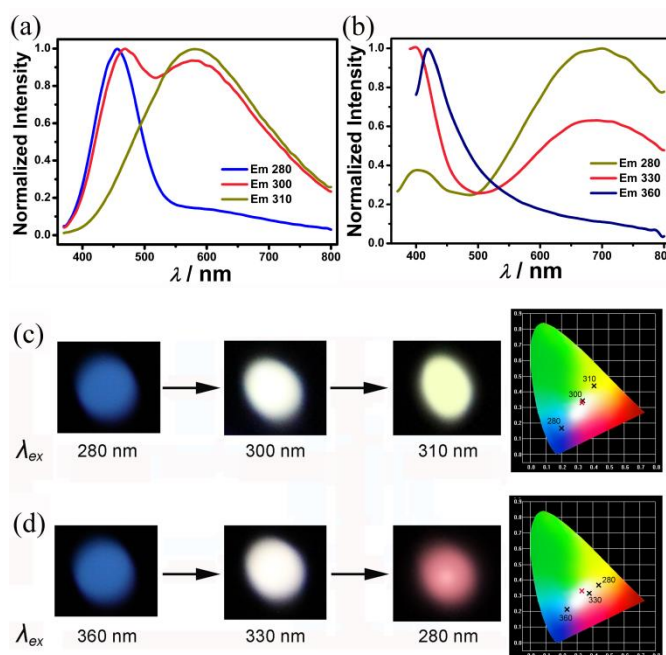


Fig. 3. Normalized solid-state photoluminescent spectra of **1** (a) and **2** (b) at room temperature by variation of excitation light; Optical photographs of **1** (c) and **2** (d) excited by different wavelengths; CIE-1931 chromaticity diagram showing the emissions excited at 280, 300, and 310 nm for **1** (c), as well as 280, 330, and 360 nm for **2** (d), red cross showing the position of pure white-light (0.33, 0.33).

High CRI white-light emitting material is very important for high-quality lighting. Here we show a possible way to create high CRI single-component white-light emitting material by organic and inorganic hybrid strategy. Compound **1** exhibits two emission peaks, centered at 455 (narrow peak, blue) and 585 nm (broad peak, yellow), respectively (Fig. 3a). These two emissions should belong to different emitting centers due to the following two reasons. 1) They have different maximum excitation (Fig. S8): the blue one has maximum excitation at 280 nm while the yellow one at 320 nm. 2) They have different lifetimes (See experimental section and Fig. S9 in the ESI): 2.89 ns for 455 nm and 18.85 ns for 585 nm, respectively. Adjusting excitation from 280 to 320 nm results the intensity of emission peak at 455 nm decreases, while that at 585 nm increases. In this way, the emission of **1** can be modulated from blue to yellow. An intermediary excitation, 300 nm, is found to produce the “best” white-light emitting with a quantum yield of 2.5%. The Commission Internationale de l’Eclairage (CIE) chromaticity coordinates of this white-light emission is (0.33, 0.34), which is very close to that of pure white light (0.33, 0.33) (Fig. 3c). The correlated color temperature (CCT) is 5393 K, corresponding to “cold” white light. Notably, the white-light emitting of **1** shows a CRI value of 96. As far as we know, this value is the highest one in the reported single component white-light emitting compound, and well above the value for fluorescent light sources (~65) and reaches the value created by expensive multi-component phosphor.

Similarly, compound **2** also has two emitting centers that locate at 420 (narrow peak, blue) and 690 nm (broad peak, orange) with lifetime of 1.98 and 54.13 ns, respectively. It

shows tunable photoluminescence from blue to orange by variation of excitation light (Fig. 3b, 3d). The maximum excitation for the blue and orange emission is at 310 and 370 nm, respectively (Fig. S10). Exciting compound **2** with the light between the two maximum excitations can obtain a balanced ratio of blue and orange emission to produce white-light emitting. The “best” excitation for white-light emitting of **2** is 330 nm. At this excitation, the CIE chromaticity coordinates and quantum yield of the white-light emission are (0.38, 0.31) and 1%, respectively (Fig. 3d). Different from **1**, compound **2** shows a “warm” white light emission with a CCT value of 3496 K that is more preferred for indoor illumination. Its CRI is 88, less than that of **1**, but very close to the value for high-level applications.

Additionally, the PXRD and emission spectra of the two compounds are similar to their as synthesized ones, which indicate these two compounds are stable at 280 °C (Fig. S11–13). **1** and **2** are also stable under photo-excitation, the intensity and peaks of the white light emission after constant irradiated for 48 h is close to that measured for their pristine samples (Fig. S14).

It has been well known that if the emission originates from the deep defects of a material, it will strongly depend on particle size and will be readily quenched by particle aggregation.¹⁵ In **1** and **2**, similar emission spectra from larger than 10 μm-sized particles of hand grinded powder and 2~3 μm-sized particles of ball-milled powder were observed (Fig. S15–S18). The emission centers are the same, only with a small difference of relative intensity. This indicates that the size of the sample has little influence to the emission, and the white-light emission of **1** and **2** is a bulk effect and not a result of surface defects.^{9a}

The short lifetimes within ns range for all of the emitting peaks of **1** and **2** indicate their fluorescence characteristic. To better understand the photoluminescent mechanisms, the emissions of H₂(DABCO)Cl₂, [Et₂DABCO]I₂ (see Experimental section and Fig. S19–S20 in the ESI) and bulk PbCl₂ were investigated, respectively. As shown in Fig. S21–S22, H₂(DABCO)Cl₂ displays a blue light emission centered at ~435 nm with lifetime of 1.85 ns when excited at 370 nm; and [Et₂DABCO]I₂ also shows a blue light emission centered at 415 nm with a lifetime of 2.20 ns when excited at 345 nm. The positions and lifetimes of these emissions are comparable to the blue light emissions in **1** and **2**, demonstrating the blue emissions in **1** and **2** originate from their organic components, respectively. Bulk PbCl₂ shows broad yellow light emission with a maximum peak at 545 nm and lifetime of 4.70 ns (Fig. S22c, S23), which is similar to the yellow / orange emission in **1** and **2**. These emissions can be assigned to a Pb-centered transition involving the *s* and *p* metal orbital.¹⁶ Owing to serious structure distortion between ground and excited state, the emission of *s*² compound shows large shift from absorption maxima, which has also been observed in **1** and **2**. The calculated energy between *s* and *p* orbital of Pb²⁺ in compound **2** is smaller than that of compound **1** (Fig. S24), in according with the red shift emission of compound **2**. The inorganic 3-D structures in **1** and **2** play very important roles in showing such

low energy emissions. Because (Me₂DABCO)₂(PbCl₆) has similar organic cation but 0-D inorganic counterpart, which only shows blue emission from organic part by varying excitation (Fig. S25–S26). The mechanism of white-light emitting in **1** and **2** is different from that of the recently reported 2-D layered hybrid perovskites (N-MEDA)[PbBr_{4-x}Cl_x] and (EDBE)[PbX₄].^{9a,9b} In these 2-D layered hybrid perovskites, the dielectric mismatch between organic and inorganic layers results multilayer quantum well structures and creates strongly bound exciton associated with the inorganic semiconducting layer. A broad distribution of intrinsic emissive trap states and strong electron-phonon coupling originated from deformable lattice in the 2-D layered inorganic structure produce very broad emission for white light. So their white-light emitting has only contribution from inorganic component, and the highest CRI in these compounds is reported 85. In our case, the white light emission is derived from the synergetic work of inorganic and organic parts. The best advantage of our compounds is that the emitting of inorganic and organic components is relatively independent. The ratio of the emitting from inorganic and organic components could be flexibly tuned to enable us to produce white light with ultra-high CRI.

Conclusions

In conclusion, two single-component white-light emitting hybrids have been reported in this work. One of them shows the highest CRI of 96 in single component phosphors to date. Their 3-D inorganic framework structures are unusual and play very important role in conducting properties and suitable long wavelength emitting for white light. The blue emitting of organic component and yellow / orange emitting of inorganic component are independently tunable to produce high CRI. Notably, compounds **1** and **2** also show multi-color emission, which may meet the requirement in colorful lighting or display. In the future, lighting system with low cost, long life, and high CRI are required for accurately mimicking lighting conditions outside. Our work shows a new method to develop high performance white phosphors with systematically tunable emission properties.

Acknowledgements

This work was financially supported by the Financial support from the NSF of China (51402293, 21401193, 21471149, 21373225), and the NSF of Fujian Province (2014J01065, 2014J07003).

Notes and references

- (a) K. Wooseok and J. Jing, *J. Am. Chem. Soc.* 2008, **130**, 8114–8115; (b) D. F. Sava, L. E. S. Rohwer, M. A. Rodriguez and T. M. Nenoff, *J. Am. Chem. Soc.* 2012, **134**, 3983–3986.
- (a) L. Chen, K.-J. Chen, S.-F. Hu and R.-S. Liu, *J. Mater. Chem.* 2011, **21**, 3677–3685; (b) A. A. Setlur, W. J.

- Heward, Y. Gao, A. M. Srivastava, R. G. Chandran and M. V. Shankar, *Chem. Mater.* 2006, **18**, 3314–3322; (c) Y. Li, A. Rizzo, R. Cingolani and G. Gigli, *Adv. Mater.* 2006, **18**, 2545–2548; (d) X.-H. Zhu, J. Peng, Y. Cao and J. Roncali, *Chem. Soc. Rev.* 2011, **40**, 3509–3524; (e) N. Guo, H. You, Y. Song, M. Yang, K. Liu, Y. Zheng, Y. Huang and H. Zhang, *J. Mater. Chem.* 2010, **20**, 9061–9067.
- 3 (a) M. Roushan, X. Zhang and J. Li, *Angew. Chem. Int. Ed.* 2012, **51**, 436–439; (b) C.-C. Shen and W.-L. Tseng, *Inorg. Chem.* 2009, **48**, 8689–8694; (c) S. Sapra, S. Mayilo, T. A. Klar, A. L. Bogach and J. Feldmann, *Adv. Mater.* 2007, **19**, 569–572.
- 4 (a) S. Ye, F. Xiao, Y. X. Pan, Y. Y. Ma and Q. Y. Zhang, *Mater. Sci. Eng. R* 2010, **71**, 1–34. (b) J. Silver, R. Withnall and A. Kitai, *John Wiley & Sons: Chichester* 2008, p 75.
- 5 (a) M.-S. Wang, S.-P. Guo, Y. Li, L.-Z. Cai, J.-P. Zou, G. Xu, W.-W. Zhou, F.-K. Zheng and G.-C. Guo, *J. Am. Chem. Soc.* 2009, **131**, 13572–13573; (b) G.-P. Yong, Y.-M. Zhang, W.-L. She and Y.-Z. Li, *J. Mater. Chem.* 2011, **21**, 18520–18522; (c) Y. Liu, M. Pan, Q.-Y. Yang, L. Fu, K. Li, S.-C. Wei and C.-Y. Su, *Chem. Mater.* 2012, **24**, 1954–1960; (d) K. T. Kamtekar, A. P. Monkman and M. R. Bryce, *Adv. Mater.* 2010, **22**, 572–582; (e) M. C. Gather, A. Köhnen and K. Meerholz, *Adv. Mater.* 2011, **23**, 233–248; (f) Z.-F. Liu, M.-F. Wu, S.-H. Wang, F.-K. Zheng, G.-E Wang, J. Chen, Y. Xiao, A.-Q. Wu, G.-C. Guo and J.-S. Huang, *J. Mater. Chem. C* 2013, **1**, 4634–4639; (g) X. Fang, M. Roushan, R. Zhang, J. Peng and H. Zeng, *Chem. Mater.* 2012, **24**, 1710–1717; (h) H.-B. Xu, X.-M. Chen, Q.-S. Zhang, L.-Y. Zhang and Z.-N. Chen, *Chem. Commun.* 2009, 7318–7320; (i) S. Dang, J.-H. Zhang and Z.-M. Sun, *J. Mater. Chem.* 2012, **22**, 8868–8873; (j) M. Shang, C. Li, J. Lin, *Chem. Soc. Rev.* 2014, **43**, 1372–1386.
- 6 (a) X.-H. Zhu, J. Peng, Y. Cao and J. Roncali, *Chem. Soc. Rev.* 2011, **40**, 3509–3524; (b) R. M. Adhikari, L. Duan, L. Hou, Y. Qiu, D. C. Neckers and B. K. Shah, *Chem. Mater.* 2009, **21**, 4638–4644; (c) Y. Liu, M. Nishiura, Y. Wang and Z. Hou, *J. Am. Chem. Soc.* 2006, **128**, 5592–5593.
- 7 Y. J. Tung, M. M. H. Lu, M. S. Weaver, M. Hack and J. J. Brown, *Proc. SPIE* 2004, **5214**, 114–123.
- 8 M. S. Park, H. J. Park, O. Y. Kim and J. Y. Lee, *Org. Electron.* 2013, **14**, 1504–1509.
- 9 (a) E. R. Dohner, A. Jaffe, L. R. Bradshaw and H. I. Karunadasa, *J. Am. Chem. Soc.* 2014, **136**, 13154–13157; (b) E. R. Dohner, E. T. Hoke and H. I. Karunadasa, *J. Am. Chem. Soc.* 2014, **136**, 1718–1721; (c) C.-Y. Sun, X.-L. Wang, X. Zhang, C. Qin, P. Li, Z.-M. Su, D.-X. Zhu, G.-G. Shan, K.-Z. Shao, H. Wu and J. Li, *Nat. Commun.* 2013, **4**, 1–8.
- 10 (a) D. B. Mitzi, S. Wang, C. A. Feild, C. A. Chess and A. M. Guloy, *Science* 1995, **267**, 1473–1476; (b) D. B. Mitzi, K. Chondroudis and C. R. Kagan, *IBM J. Res. Dev.* 2001, **45**, 29–45; (c) N. Leblanc, W. Bi, N. Mercier, P. Auban-Senzier and C. Pasquier, *Inorg. Chem.* 2010, **49**, 5824–5833.
- 11 (a) Z.-J. Zhang, S.-C. Xiang, G.-C. Guo, G. Xu, M.-S. Wang, J.-P. Zhou, S.-P. Guo and H.-S. Huang, *Angew. Chem. Int. Ed.* 2008, **47**, 4149–4152; (b) D. B. Mitzi, *Prog. Inorg. Chem.* 1999, **48**, 1–121; (c) J. D. Martin and K. B. Greenwood, *Angew. Chem. Int. Ed.* 1997, **36**, 2072–2075.
- 12 (a) G.-E Wang, X.-M. Jiang, M.-J. Zhang, H.-F. Chen, B.-W. Liu, M.-S. Wang and G.-C. Guo, *CrystEngComm* 2013, **15**, 10399–10404; (b) G.-E Wang, M.-S. Wang, X.-M. Jiang, Z.-F. Liu, R.-G. Lin, L.-Z. Cai, G.-C. Guo and J.-S. Huang, *Inorg. Chem. Commun.* 2011, **14**, 1957–1961; (c) G. Xu, G.-C. Guo, J.-S. Huang, S.-P. Guo, X.-M. Jiang, C. Yang, M.-S. Wang and Z.-J. Zhang, *Dalton Trans.* 2010, **39**, 8688–8692; (d) G. Xu, G.-C. Guo, M.-S. Wang, Z.-J. Zhang, W.-T. Chen and J.-S. Huang, *Angew. Chem. Int. Ed.* 2007, **46**, 3249–3251; (e) G. Xu, Y. Li, W.-W. Zhou, G.-J. Wang, X.-F. Long, L.-Z. Cai, M.-S. Wang, G.-C. Guo, J.-S. Huang, G. Bator and R. Jakubas, *J. Mater. Chem.* 2009, **19**, 2179–2183.
- 13 (a) M. Z. Liu, M. B. Johnston and H. J. Snaith, *Nature* 2013, **501**, 395–398; (b) J. Burschka, N. Pellet, S.-J. Moon, R. Humphry-Baker, P. Gao, M. K. Nazeeruddin and M. Gratzel, *Nature* 2013, **499**, 316–319; (c) H. Zhou, Q. Chen, G. Li, S. Luo, T. Song, H.-S. Duan, Z. Hong, J. You, Y. Liu and Y. Yang, *Science* 2014, **345**, 542–546; (d) N. J. Jeon, J. H. Noh, Y. C. Kim, W. S. Yang, S. Ryu and S. Il Seok, *Nature Mater.* 2014, **13**, 897–903.
- 14 (a) A. Jaffe, Y. Lin, W. L. Mao and H. I. Karunadasa, *J. Am. Chem. Soc.* 2015, **137**, 1673–1678; (b) Z. Xu, D. B. Mitzi, C. D. Dimitrakopoulos and K. R. Maxcy, *Inorg. Chem.* 2003, **42**, 2031–2039; (c) C. C. Stoumpos, C. D. Malliakas and M. G. Kanatzidis, *Inorg. Chem.* 2013, **52**, 9019–9038.
- 15 M. J. Bowers, J. R. McBride and S. J. Rosenthal, *J. Am. Chem. Soc.* 2005, **127**, 15378–15379.
- 16 R Kink, T Avarmaa, V Kisand, A Lõhmus, I Kink and I Martinson, *J. Phys.: Condens. Matter* 1998, **10**, 693–700.